Available online at www.sciencedirect.com
SCIENCE DIRECT
Journal of Catalysis 239 (2006) 162–172
JOURNAL OF CATALYSIS
www.elsevier.com/locate/jcat

Influence of water and pretreatment conditions on CO oxidation over $Au/TiO_2–In_2O_3$ catalysts

M.A. Debeila, R.P.K. Wells, J.A. Anderson *

Surface Chemistry and Catalysis Group, Department of Chemistry, King's College, University of Aberdeen, AB24 3UE, Scotland, UK

Received 14 December 2005; revised 23 January 2006; accepted 24 January 2006

Available online 21 February 2006

Abstract

The catalytic activity of $Au–TiO_2–In_2O_3$ catalyst in the oxidation of CO in the presence and absence of added water vapour and using different pretreatment conditions was tested and compared with that of a $Au–TiO_2$ sample prepared using a commercial support used as a reference catalyst. The $Au–TiO_2–In_2O_3$ samples showed less activity than the standard $Au–TiO_2$ sample but could be reused after reaction up to 500 °C without loss of activity. The activity of $Au–TiO_2–In_2O_3$ catalysts for CO oxidation was relatively insensitive to the pretreatment procedures but showed quite distinct light-off curves compared with those of $Au–TiO_2$. Differences between the catalytic behaviour of the two Au-supported catalysts indicate differences in the relative ease by which the oxides become dehydroxylated by thermal treatments. Results for $Au–TiO_2–In_2O_3$ are consistent with a scheme in which at low temperatures ($\leqslant$264 °C), CO_2 formation involves gold sites with participation of hydroxyl groups of the support. Above this temperature, dehydroxylation of the support leaves the gold component with low activity, and the rate of CO_2 formation becomes equivalent to the rate obtained over the support alone. Cooling the samples back to room temperature recovers the initial activity of the gold, confirming that deactivation is completely reversible. Experiments conducted involving deliberate addition of water show that the deactivation caused by an excess of H_2O for both $Au–TiO_2$ and $Au–TiO_2–In_2O_3$ is also reversible, and that the extent to which water is retained is quite different for the two catalysts. Reaction mechanisms, taking into account the involvement of H_2O, are discussed.

Keywords: $Au/TiO_2–In_2O_3$ catalysts; CO oxidation; Influence of water; Gold catalysis

1. Introduction

Following the observation in the late 1980s that gold in the form of small particles displays significant catalytic properties [1], the activity of gold has become widely recognised for various reactions [2,3]. Catalytic properties of these gold nanoparticles depend on particle size, the nature of the oxide support material, the interaction between gold nanoparticles and the support oxide, and the shape of the gold nanoparticles [2,4,5]. Despite high initial activity, gold catalysts often deactivate with time on line [6–9]. This deactivation has been attributed to sintering of gold during reaction [10], reduction of oxidic gold to metallic gold [11], accumulation of carbonate on the surface [9,12] and the presence of moisture [13]. It has been suggested that the effect of the oxidation state of gold is about as important as that of the particle size of metallic gold [14]. The issue of active sites is receiving considerable attention and remains a matter of debate [15–17]. Some authors suggest that oxidic gold is more active [18], whereas others suggest that metallic gold is more active than oxidic gold [8,19]. The presence of both metallic and oxidic gold has been detected in working catalysts [20]. This may be due to the fact that the activity of supported gold particles varies with pretreatment. This is another controversial issue, because there is no general agreement on the optimal calcination temperature for the supported gold particles for CO oxidation [2,5,21,22]. However, it is generally observed that calcination at high temperature results in a catalyst with low activity. This has been attributed to sintering [23] and/or a change in particle shape [24]. The activity of $Au–TiO_2$ has been compared after pretreatment in different gas atmospheres; one study found that reduction gave a catalyst with higher activity than oxidized catalyst [25], whereas another reported that specific reduction–oxidation pre-

* Corresponding author.
E-mail address: j.anderson@abdn.ac.uk (J.A. Anderson).

0021-9517/$ – see front matter
doi:10.1016/j.jcat.2006.01.028

treatment resulted in active catalyst [26]. Recently, using appropriate thermal pretreatment, Au–Fe_2O_3 catalysts were able to achieve high selectivity in the competitive oxidation of CO in the presence of excess H_2, H_2O, and CO_2 [27]. The two-step calcination was thought [27] to result in the removal of residual cationic gold that is otherwise active for the reverse water–gas shift reaction, which would otherwise limit the overall conversion of CO.

In terms of moisture sensitivity, some researchers report positive [14] and others report negative [7,8,13,28] effects of moisture on the activity of supported gold catalysts. In fact, previously proposed reaction mechanisms [29] include the role of hydroxyl groups. It has been shown that for Au–TiO_2(P25), the amount of moisture adsorbed by the catalyst is key to explaining the differences observed [30]. The rate of CO oxidation as a function of moisture content takes the form of a curve that passes through a maximum and gives low activity at high moisture content due to the blocking of active sites by water [30]. The ability of supported gold catalysts to tolerate water contents of the order of 0–10 vol% and at temperatures around 80 °C is essential if these catalysts are to find application in preferential CO oxidation from hydrogen-containing feed-streams (PROX) for polymer electrolyte fuel cell applications [27].

Composite oxide supports have been successfully applied to stabilize small metal particles, although introduction of a second oxide component into TiO_2 also causes surface modification that may modify activity [31], particularly if interfacial sites are involved in the reaction. Addition of In_2O_3 is expected to modify interfacial sites and expose Lewis acid sites of dissimilar character to those of titania; these may be influential in activating water molecules, which are suspected to play a key role over Au/TiO_2 [28]. In the present study, a composite TiO_2–In_2O_3 support was prepared, and the sensitivity to pretreatment conditions and to the influence of water vapour in the CO oxidation reaction was tested.

The catalytic behaviour of this sample was compared with a sample of equivalent Au loading (2%) but using Degussa P25 as a support, because the later can be considered a benchmark for reference purposes and the moisture sensitivity for CO oxidation has been reported previously [30].

2. Experimental

2.1. Preparation of Au–TiO_2

TiO_2 (Degussa P25) was suspended in 180 cm^3 of distilled water at room temperature and stirred. Then 4 cm^3 of $HAuCl_4$ [2.538×10^{-2} M] was added, and the mixture was stirred continuously. Subsequently, 4 cm^3 of KOH solution (0.2 M) was added, and stirring continued for another 10 min. The catalyst was separated from the supernatant liquor by centrifugation, and the powder was dried at ca. 120 °C and ground before use. A portion of the catalyst was washed, and the washings were tested for chloride ion using $AgNO_3$. No evidence of chloride was found. The nominal loading was 2%, although ICP-MS revealed the final catalyst had a loading of 1.9 wt% gold.

2.2. Preparation of TiO_2–In_2O_3 support

A 1.0-g sample of titanium *n*-butoxide diluted with 7.5 cm^3 of ethanol was placed in a round-bottomed flask and heated under reflux to 70 °C under constant stirring. Then 0.2 cm^3 of nitric acid was added as hydrolysis catalyst and allowed to continue for 10 min before the dropwise addition of an aqueous solution of $In(NO_3)_3$ (calculated to provide a 5 wt% loading of indium oxide in the final support). Water was then added until gelling occurred. The system was then maintained under reflux for 3 h at 70 °C, followed by drying of the gel thus obtained in an oven at 70 °C. The sample was then calcined at 400 °C for 4 h in a flow of air (100 cm^3 min^{-1}).

2.2.1. Preparation of Au–TiO_2–In_2O_3

The Au–TiO_2–In_2O_3 was prepared by a deposition–precipitation method, using $HAuCl_4 \cdot H_2O$ as a source of gold. A gold solution was prepared using the gold precursor in deionised water and by adding ammonia solution at room temperature to give a final pH of 7. The choice of this pH was based on selection of a value between 6 and 10 whereby partially hydrolysed $[Au(OH)_nCl_{4-n}]^-$ ($n = 1$–3) is formed, which can then react with the support surface [3]. The support was added and suspended in this solution, and the mixture was stirred for another 30 min. The sample was aged for 24 h and filtered, after which the solid slurry was washed with deionised water several times and dried overnight in an oven at 120 °C. Analysis by ICP-MS revealed that the final catalyst had a gold loading of 1.8 wt% even though the nominal loading was 2%.

2.3. DRIFT and activity tests

Samples (50 mg) were loaded into a DRIFTS cell with CaF_2 windows and a heating system that allowed operation under different atmospheres at temperatures up to 600 °C. Spectra (resolution, 4 cm^{-1}; average of 50 scans) were recorded with a Perkin-Elmer 1720 FTIR. Inlet gases were provided via a computer-controlled gas blender, and exit gases from the DRIFS cell were monitored using a Baltzers Prisma QMS. All inlet and outlet lines were heated using external heating tape to avoid condensation of water. Catalyst pretreatment involved heating in air, N_2, or H_2 (gas flow, 40 ml/min) for 30 min at the desired temperature, followed by cooling to room temperature and exposure to the reactant gas mixture (CO 1%, air 4.7%, balance N_2). For light-off experiments, samples were heated at 6.7 °C min^{-1} to 500 °C while simultaneously recording DRIFT spectra and monitoring the m/e signals. Pretreatment of the samples involved in situ calcination at different temperatures (200 and 300 °C), denoted as C200 and C300, respectively. Other pretreatment involved heating in flowing N_2 at 200 °C; this sample is denoted as C200N_2. Some of the catalysts were also prereduced at 200 °C in H_2 postcalcination; these are denoted as C300R200 and C200R200. The dried sample prereduced in H_2 using uncalcined catalyst is denoted as R200. Pretreatment of the support involved prereduction in H_2 at 200 °C; this is denoted as support R200.

To test the stability of the gold catalyst under selected reaction conditions, and also to study the influence of cooling in different gas atmospheres, several reactions were performed by conducting cycles of experiments. Fresh sample was loaded into the cell and pretreated in flowing nitrogen. After cooling to room temperature, the reactant mixture was introduced. At the end of the first run, the reaction mixture was replaced by flowing N_2 (at 500 °C), and the sample was cooled to room temperature before introducing the reacting mixture and performing the second run. In the case of Au–TiO_2–In_2O_3, after the first run and cooling of the sample in N_2, CO was introduced for 5 min at room temperature before the introduction of air. The activity measurement was carried out as before to generate the second curve (second run). Again at the end of the second run, flowing N_2 was introduced and the sample was cooled to room temperature. Similar procedures were followed to generate the activity curve for the third run. In another experiment, the sample was cooled in air instead of N_2, and the activity profile was carried out as in the first run.

For experiments involving the use of water, 100 μl was injected by syringe into the reactant stream, where the gases were preheated above 110 °C to avoid condensation. The effect of this additional water was then monitored as a function of time under isothermal conditions at 70 °C. Laser Raman spectra were obtained using a Renishaw *InVia* Microscope at 633 nm excitation.

3. Results

3.1. Au–TiO_2 (P25)

3.1.1. Temperature-dependent activity

Fig. 1 depicts the temperature-dependent activity of the 2 wt% Au–TiO_2 catalyst at 25–500 °C. The profile shows an initial 50% CO conversion at room temperature, rising to around 90% at around 150 °C. The sample was cooled in 100% N_2 flow after the first experiment to test the stability of the catalyst under the conditions used. Comparing the two curves shows that in the second run, a higher initial activity was obtained and the onset of light-off was reduced by ca. 16 °C relative to the first run, showing that the catalyst had been further activated either during the reaction or by the cooling process in nitrogen.

The differences in measured activities at 40 °C are shown in Table 1. The relative difference in activity between consecutive runs decreased with increasing temperatures (or conversion), and the two curves coincide at ca. 400 °C (Fig. 1). Apart from the separation with respect to temperature/conversion, the shapes of the two profiles (first and the second runs) are almost identical; that is, the curves consist of a sharp rise in activity up to ca. 170 °C, followed by a modest increase and then a levelling-off at temperatures above 300 °C.

3.1.2. Influence of water

Fig. 2 shows the impact of water on the conversion profile for the CO oxidation over the 2-wt% Au–TiO_2. The sample was heated to 70 °C in a flow of CO/air/N_2; this temperature was chosen because the catalyst shows activity at this temperature

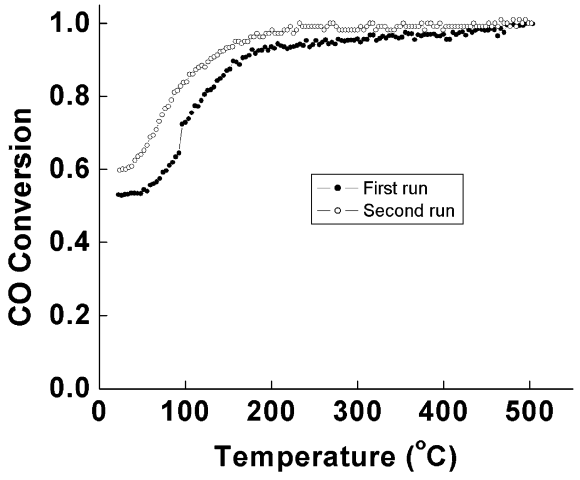

Fig. 1. CO conversion as a function of temperature over uncalcined 2 wt% Au–TiO_2.

Table 1
Comparison of catalytic activities obtained for the different samples and after different pre-treatment conditions

Catalyst	Pretreatment	Reaction temperature (°C)	Activity (mol g_{cat}^{-1} s^{-1})
2.4%Au/TiO_2 [7]	Calcined at 400 °C	40	0.63×10^{-6}
1.8% Au/SiO_2 [3]	Reduced at 450 °C	40	6.9×10^{-8}
1.9% Au/TiO_2 (P25)	Uncalcined	40	7.4×10^{-6}
1.9% Au/TiO_2 (P25)	After CO oxidation to 500 °C	40	9.7×10^{-6}
1.8%Au/TiO_2–In_2O_3	Calcined at 200 °C	40	4.2×10^{-6}
1.8%Au/TiO_2–In_2O_3	Nitrogen at 200 °C	40	3.57×10^{-6}
1.8%Au/TiO_2–In_2O_3	Calcined at 300 °C	40	3.72×10^{-6}
1.8%Au/TiO_2–In_2O_3	Reduced at 200 °C	40	3.57×10^{-6}
1.8%Au/TiO_2–In_2O_3	Calcined 200, then reduced at 200 °C	40	3.72×10^{-6}
1.8%Au/TiO_2–In_2O_3	Calcined 300, then reduced at 200 °C	40	4.5×10^{-6}

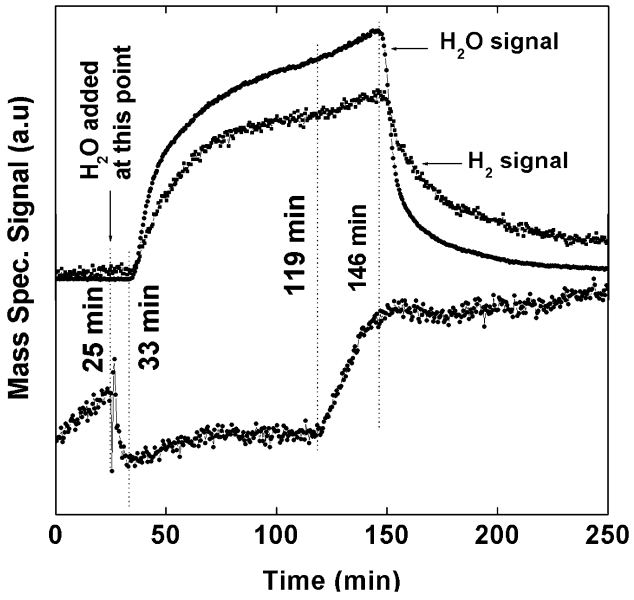

Fig. 2. Influence of H_2O on CO oxidation activity ($m/e = 44$ trace for CO_2) over uncalcined 2 wt% Au–TiO_2.

(Fig. 1) and because operation in PEM fuel cell applications requires temperatures of ca. 80 °C. Fig. 2 also shows the corresponding mass spectrometer H_2O and H_2 signals. Soon after the injection of water into the gas stream, water began to adsorb onto the catalyst surface, accompanied by a rapid decrease in CO oxidation activity. After 33 min, the activity reached its lowest value under wet conditions (but retained some activity). Between 25 and 33 min, the H_2O and H_2 signals remained constant (Fig. 2). Note that the mass spectrometer signal gives the concentration of the species in the exit stream, so that while H_2O was being adsorbed onto the surface, the concentration of H_2O or H_2 in the exit stream exhibited no change in concentration, as indicated by constant values up to 33 min (Fig. 2). From 33 to 119 min, the activity (CO_2 formation) was fairly low but showed a gradual recovery. Within this time interval there was a sharp increase in the concentrations of H_2O and H_2 in the exit stream, which, after some time, reached a plateau at the 119-min point. Beyond this point, the H_2O/H_2 signals showed modest increases, and the CO oxidation activity recovered to above its original value and then remained roughly constant beyond the 146-min point. Interestingly, after 146 min (i.e., after the CO oxidation activity had reached a maximum), there was a rapid decrease in the H_2O signal, followed by a further modest decrease up to ca. 228 min, after which the signal remained constant. Similar (although slightly less pronounced) features were observed in the H_2 signal (see Fig. 2). The H_2O and H_2 profiles were always roughly similar, with a change in the H_2O signal in the exit stream being accompanied by a change in the H_2 signal.

3.2. $Au–TiO_2–In_2O_3$

3.2.1. Sample characterization

Nitrogen adsorption–desorption isotherms show that the $TiO_2–In_2O_3$ has a mesoporous structure, with an average pore radii of 3 nm. The BET area of the catalysts after calcination was 100 $m^2\,g^{-1}$. XRD patterns for $TiO_2–In_2O_3$ showed only peaks due to TiO_2 (anatase), indicating that In_2O_3 was either present as small crystallites or as an amorphous phase, or with In ions exchanged into the TiO_2 lattice. No additional features were detected by the same technique after addition of gold. Possible evidence of incorporation of In exchange into the titania lattice was the inhibition of the anatase to rutile-phase transformation, which had not occurred after heating to 600 °C, whereas pure TiO_2 underwent this phase transition at the same temperature. Raman spectra of the $Au–TiO_2–In_2O_3$ sample (Fig. 3) exhibit a clear 7-cm^{-1} shift in the E_{1g} signal at 142 cm^{-1} for an anatase standard. Although this could be attributed to a change in particle size, it is equally likely that the changes in band position of the E_{1g} signal and bandwidth of all of the anatase signals result from changes in lattice parameters caused by substitution of In_2O_3 into the TiO_2 structure. In either case, the In is clearly highly dispersed though the titania matrix, which should maximise its effect on the surface properties of the support material. TGA (not shown) exhibited a weight loss due to water at 75–150 °C, representing ca. 5% of the total sample mass. At 150–350 °C, the weight loss was less

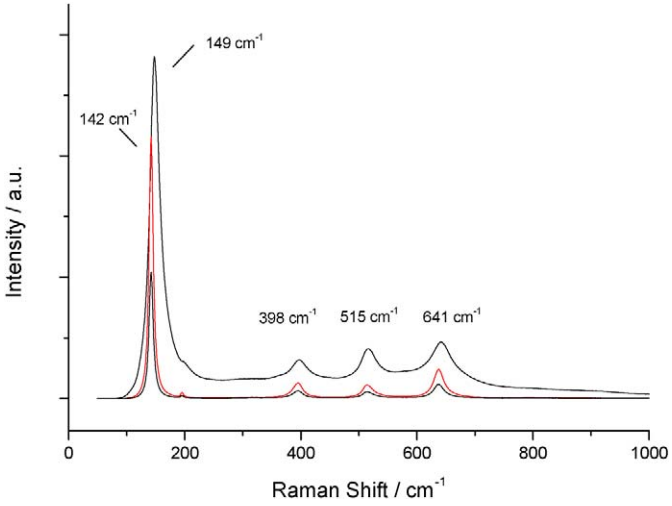

Fig. 3. Laser Raman spectra (633 nm excitation) showing an anatase standard (lower two traces) and the $TiO_2–In_2O_3$ sample (upper plot).

significant, giving a total of ca 7%. Increasing the temperature to 500 °C caused only slight further loss (ca 1%). The gold-containing sample was exposed to CO at 25 °C after evacuation at the same temperature. Adsorbed CO could not be detected by FTIR under these conditions.

3.2.2. Influence of pretreatment

Table 1 summarises the influence of pretreatment on catalytic activities at 40 °C and also compares activities obtained with the Au/TiO_2 (P25) and with data for supported Au catalysts from the literature. Fig. 4a shows the activities for the 2-wt% $Au–TiO_2–In_2O_3$ catalyst preoxidized in air before activity measurements. Fig. 4b shows the same for catalysts reduced after calcination and others directly reduced without precalcination or pretreated in a N_2 flow. In general, the activities of the $Au–TiO_2–In_2O_3$ catalysts were inferior to those of $Au–TiO_2$, and the temperature/conversion plots display profile shapes quite unlike those of the $Au–TiO_2$ catalysts (Fig. 1). The profiles show an initial sharp rise up to ∼93 °C (region I), followed by gradually increasing conversion (region II) up to ∼300 °C, then a steeper rise in activity (region III) and finally a plateau above 361 °C.

To account for the profile shapes and to determine the extent of reactions occurring on the support material alone, the support was studied under identical conditions (Fig. 4b). Below 264 °C, the activity was less than that of $Au–TiO_2–In_2O_3$, but it rose slowly with increasing temperature until the onset of a sharp rise in conversion at 264 °C. At around 300 °C, the activity curve for the support coincided with those of $Au–TiO_2–In_2O_3$; this continued to 361 °C, at which point the activity began to level off.

Fig. 5a shows FTIR spectra of $Au–TiO_2–In_2O_3$ after pretreatment before introduction of the reaction mixture. An intense, broad band at 3500–2800 cm^{-1} in the OH-stretching region characterizes this spectrum. In the 1800–1200 cm^{-1} region, an intense band at 1630 cm^{-1} due to δ(HOH) and medium- to low-intensity bands at 1547, 1450, and 1360 cm^{-1} are seen. The former pair seems to grow together, suggesting

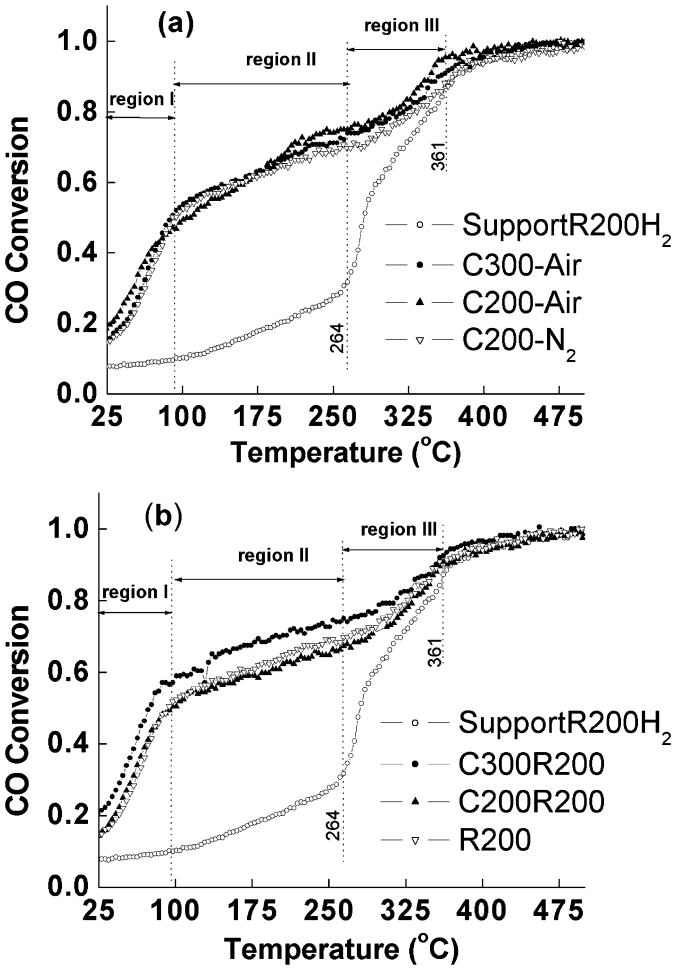

Fig. 4. (a) Temperature dependent activity curves for Au–TiO_2–In_2O_3 following pre-treatment at different temperatures and under different gaseous atmospheres. (b) Light-off curves for Au–TiO_2–In_2O_3 following calcination/reduction or reduction pre-treatment alone at different temperatures.

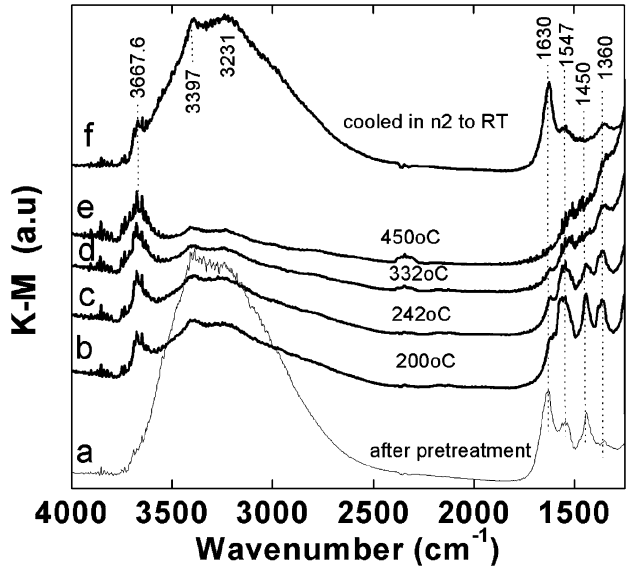

Fig. 5. FTIR spectra recorded during CO oxidation measurements over Au–TiO_2–In_2O_3: (a) after heating in N_2, and then (b–e) in CO and air at (b) 200, (c) 242, (d) 332, and (e) 450 °C, then after (f) cooling in flowing N_2 to room temperature.

that they may be due to the same surface species and correspond to bands assigned to monodentate carbonate species [7], although carboxylate species also have absorption bands in the same region, that is, ν_{asym}(OCO) at 1575–1540 cm^{-1} and ν_{sym}(OCO) at 1410–1330 cm^{-1} [7]. The band at 1450 cm^{-1} may alternatively be assigned to uncoordinated carbonate [7]. Surface formate species [32], (bands at ∼2880, 1597, and 1374 cm^{-1}) were not detected. Introducing the reaction mixture into the cell and heating to 200 °C resulted in decreasing intensity of the band due to δ(HOH) but increasing intensity of the bands due to carboxylate/carbonate species (Fig. 5b) indicating that the latter were generated during the reaction. Activity data (Fig. 4) at 200 °C showed a modest increase in CO conversion (region II). At 242 °C (Fig. 5c), the spectra showed that these surface species were slowly depleted, whereas CO conversion exhibited a moderate increase (Fig. 4). At 332 °C (Fig. 5d), almost all of the surface carboxylate/carbonate species was depleted, corresponding to the second rise in CO conversion levels (region III). Decomposition of these surface species may have contributed to the release of CO_2 at these temperatures. By 450 °C, these species decomposed completely, and the activity curve reached a plateau. In this zone, the rate of CO_2 formation on the support was comparable to that formed over Au–TiO_2–In_2O_3. Results (Fig. 4) suggest that below 300 °C, CO_2 formation may arise from reaction mainly on gold sites (or sites activated by the presence of Au), and above 300 °C, CO_2 formation arises from reactions on the support. Comparing Figs. 4 and 5 reveals that region II (Fig. 4) is characterized by enhanced carbonate/carboxylate surface species, which then decompose at above 242 °C.

3.2.3. *Introducing air/O_2 to a CO-covered surface*

Cycles of reaction were conducted over Au–TiO_2–In_2O_3 catalyst to investigate catalyst stability and also to evaluate the importance of the order of exposure of each reactant. FTIR experiments [32,33] suggest that CO and oxygen are competitively adsorbed on gold sites; thus, initial activity is expected to be different when the two reactants are introduced simultaneously rather than sequentially. In this experiment, after the first reaction run and cooling to room temperature in N_2, CO was introduced for 5 min before air was introduced at the same temperature, followed by the start of the heating ramp to generate the second curve. This was followed by cooling in N_2 and then this same procedure (i.e., introducing CO for 5 min before air) to generate the third curve. Light-off curves are displayed in Fig. 6; the corresponding H_2 and H_2O signals are depicted in Figs. 7 and 8, respectively. The CO conversion curve for the second run started at the same point as the first run (Fig. 6), however, beyond room temperature, there was a rapid increase in CO_2 formation above that observed for the first run. In the third run, CO_2 formation was observed even at room temperature as soon as the second reagent (O_2) was introduced. The second and third runs coincided almost completely above 40 °C, confirming the reproducibility of the results and the absence of irreversible deactivation. All three curves coincided at temperatures above 170 °C (Fig. 6). The similarity between runs 2 and 3 and their contrast with run 1 can also bee seen in the

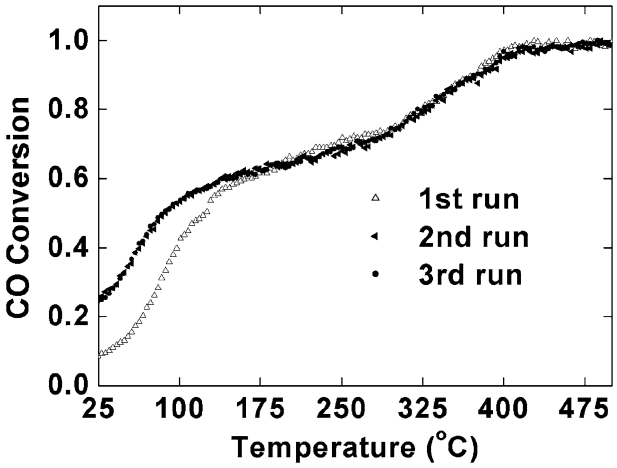

Fig. 6. Repeat light-off curves for Au–TiO_2–In_2O_3 catalyst: (i) the first run, both CO and air introduced simultaneously (ii) then cooled in N_2 before the second run, CO introduced at 20 °C for 5 min before addition of air, (iii) then cooled in N_2 and CO introduced at 20 °C for 5 min before addition of air.

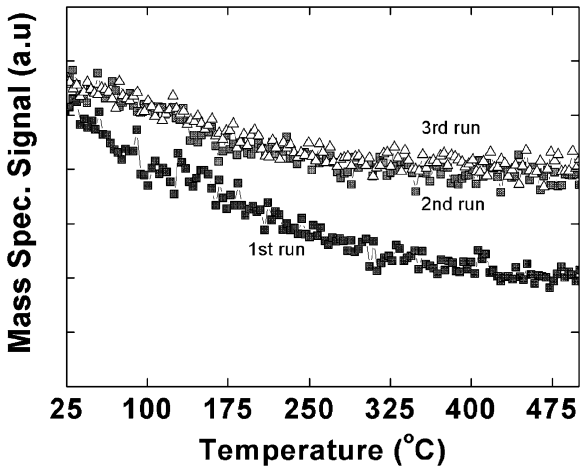

Fig. 7. MS signal due to hydrogen detected during CO oxidation (as Fig. 6) over Au–TiO_2–In_2O_3 during (i) the first run, (ii) the second run, and (iii) the third run.

hydrogen (Fig. 7) and water (Fig. 8) traces recorded as functions of temperature, hinting at a role of one or both of these in determining catalyst behaviour. CO conversion was somewhat similar to Au–TiO_2 conversion (Fig. 1) in that both catalysts exhibited improved low-temperature activity after exposure to the reaction mixture or after cooling in inert gas.

3.2.4. Effect of introducing CO to a surface pre-exposed to oxygen

Given the enhanced activity after heating in the reaction mixture and cooling in inert, the activity of Au–TiO_2–In_2O_3 was tested after a light-off test, followed by cooling in air. This procedure was adopted to determine whether the high level of initial activity after cooling in nitrogen was a consequence of starting with an Au surface in a fully reduced state, whereas cooling in air would leave the surface with a covering of oxygen. The activity curves are shown in Fig. 9; the sample after cooling in air shows greater activity than the fresh catalyst at temperatures below ca. 50 °C, but then the conversion profile

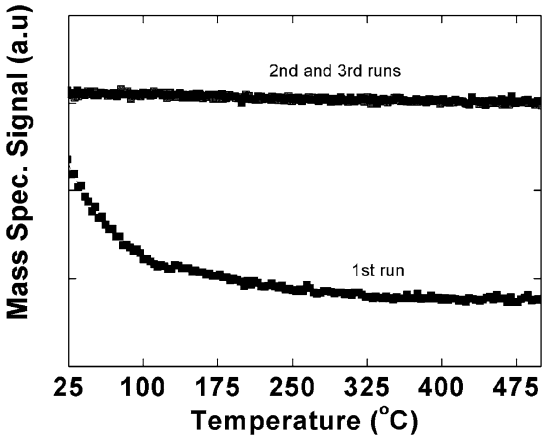

Fig. 8. MS signal due to water during CO oxidation (as Fig. 6) over Au–TiO_2–In_2O_3 during (i) the first run, (ii) the second run and (iii) the third run.

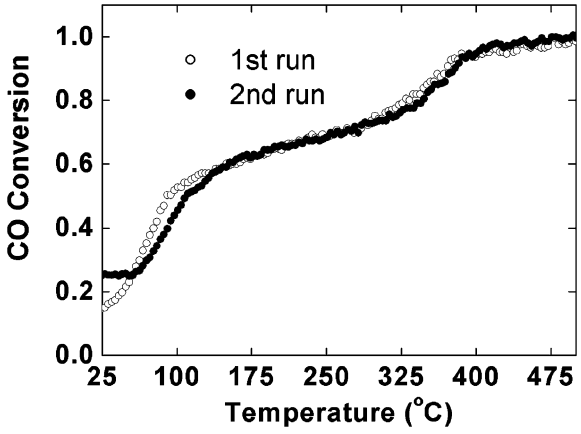

Fig. 9. Repeat light-off curves showing the effect of cooling the Au–TiO_2–In_2O_3 catalyst in air (i) the first run, both CO and air were introduced simultaneously at 20 °C, (ii) the second run, cooled in air from 500 °C to 20 °C before addition of CO and then air.

is displaced to give slightly poorer performance relative to the fresh catalyst in the range of 50–130 °C (i.e., region I). Beyond this temperature (regions II and III), the two curves coincided almost exactly. Mass spectrometry signals due to water increased with the sample at 300–500 °C (not shown) during the first run without a corresponding change in hydrogen signal. During the second run, neither water nor hydrogen signals showed an appreciable response to changes in temperature.

3.2.5. Influence of water

The influence of H_2O on CO oxidation activity over Au–TiO_2–In_2O_3 was investigated at 70 °C, a temperature corresponding to region 1, where the catalyst was active for CO but not for H_2 oxidation (Figs. 7 and 8) and where no activity was found for the support alone. The time-dependent activity showing the effect of added water on Au–TiO_2–In_2O_3 is depicted in Fig. 10 (as was shown for Au–TiO_2 in Fig. 2); corresponding FTIR spectra are shown in Fig. 11. Spectra were recorded at the times indicated by the letters shown in Fig. 10 during the collection of activity data. Fig. 10 also includes the H_2O and H_2 mass spectrometry signals. The overall shape of the formation curve

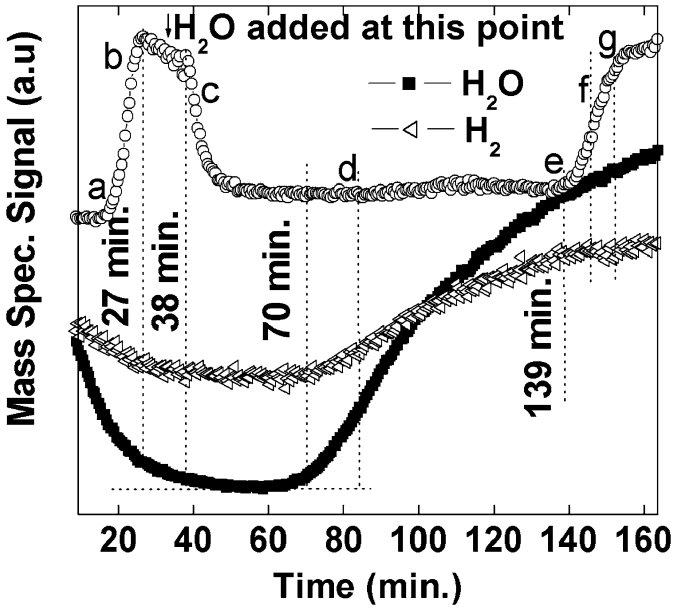

Fig. 10. Influence of H_2O on CO oxidation activity of Au–TiO_2–In_2O_3 catalyst. Heating in CO/air to 70 °C in the absence of water vapour (points a and b), after injection of water (points d, e, f, and g), and during recovery of CO oxidation activity (points e, f, and g).

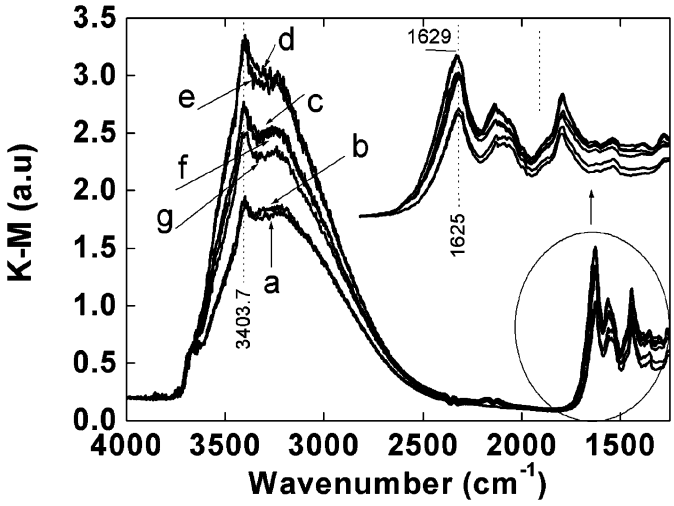

Fig. 11. In situ FTIR spectra during CO oxidation measurements showing the influence of H_2O. Spectra were recorded at times corresponding to points during the activity profiles shown in Fig. 10. Heating in CO/air to 70 °C in the absence of water vapour (points a and b), after injection of water (points d, e, f, and g), and during recovery of CO oxidation activity (points e, f, and g).

for CO_2 was generally similar to that for Au–TiO_2 (Fig. 2), with a loss in activity after injection of water (point c) but without reaching 0% CO conversion, followed by recovery after a certain time to achieve an activity level at least equivalent, if not greater, than the original. The recovery of CO oxidation activity was slightly faster for Au–TiO_2, with signs of recovery seen after 86 min (Fig. 2), compared with ca. 100 min for Au–TiO_2–In_2O_3 (Fig. 10). After the introduction of CO + air and initiation of temperature ramping, the activity increased, as shown by increased CO_2 levels. Note that although the conversion to CO_2 increased, the signals of H_2O and H_2 decreased until ca. 27 min (during dry conditions). At this point, the temperature was held constant at 70 °C, and water was added to the reaction mixture, as indicated in the figure. The 38th minute marks the onset of activity loss; after 70 min, the activity reached its lowest value under wet conditions. The corresponding H_2O and H_2 signals indicate fairly constant values during this time (38–70 min). It can be assumed that during this time, H_2O was being adsorbed by the catalyst. The breakthrough time was significantly greater (32 min) than the 8 min exhibited by the Au/TiO_2 (P25) reference sample (Fig. 2). This was confirmed in FTIR spectra (Fig. 11), in which the signal in the OH stretching region increased and reached its maximum value during this time. After 70 min, the levels of H_2O and H_2 in the exit stream began to increase, suggesting desorption of these species (H_2O and H_2) from the surface, until after 139 min, when the rate of increase of the H_2O signal diminished. The H_2 signal did not increase significantly after 139 min. At this point, the activity began to recover (Fig. 10, point e), accompanied by a decreased signal in the OH-stretching region (Fig. 11e). Because the intensity of the FTIR band at ca. 3400 cm^{-1} is related to the amount of adsorbate on the surface, it is clear that the CO oxidation activity began at a stage when the level of H_2O on the surface was still greater than it had been at the onset of the experiment; that is, the intensity at 3400 cm^{-1} at point e was greater than it was before the introduction of H_2O (compare spectra a and e in Fig. 11 and point e in Fig. 10). At point g (Fig. 10), the activity had recovered to almost original levels, although water levels on the catalyst surfaces (Fig. 11g) were still higher than those before water injection (Fig. 10a). The rise in activity to the original value (before the H_2O was added) while the adsorbed level of H_2O was still high (Fig. 11 curves b and g) and the decrease in H_2O signal during the initial rise in CO conversion (up to 27 min) suggest the possibility that H_2O- and/or H_2O-derived species are involved in reactions leading to the formation of CO_2. Decreasing levels of both H_2O and H_2 during light-off (before water injection), and the relatively constant value of the H_2 signal during recovery of CO oxidation (under wet conditions) rule out H_2 oxidation as playing a significant role under the conditions used in this study.

Results for Au–Fe_2O_3 [34] show that adding water at 80 °C not only enhanced surface carbonate levels, but also led to changes in peak frequencies. It has been suggested that water assists in the conversion of thermally stable carbonates into more labile bicarbonates, the latter of which are identified by maxima at ca. 1640, 1430, and 1221 cm^{-1} [35]. Spectra were recorded at the beginning of the reaction in dry conditions and then again under wet conditions, to determine whether such species were formed at the expense of surface carbonates. The insert in Fig. 11 shows that with the exception of the band at 1630 cm^{-1} due to δ(HOH), which increased after exposure to H_2O, in the other bands the shapes and the intensities remained fairly constant throughout the reaction. That is, no additional stable species were detected during light-off (when the activity rose under dry conditions), or when the activity dropped under wet conditions or during the recovery of CO oxidation, and, by implication, no new surface CO-containing species were formed as a result of the presence of H_2O.

4. Discussion

4.1. Activity of Au–TiO_2 (P25)

The 2-wt% Au–TiO_2 exhibited high stability, with lower [28] or higher [7] activity than reported for Au/TiO_2 (P25) (Fig. 1 and Table 1). One challenge encountered when using gold catalysts is dealing with activity loss during reactions due to particle aggregation [36,37]. The similarity in repeat light-off experiments for Au–TiO_2 here (Fig. 1) is a consequence of a stable dispersion due to the preparation procedure used. Our results confirm not only that gold particles are stable after operation at 500 °C, but also that the catalyst is further activated in the reaction mixture, as reported previously [8,25]. The activity of the Au–TiO_2 catalyst (Fig. 2) was obtained without activation, consistent with observations for Au–TiO_2 prepared by deposition–precipitation [38], where calcination had no significant effect on CO oxidation activity.

4.2. Au–TiO_2–In_2O_3

Light-off curves for Au–TiO_2–In_2O_3 (Fig. 4) were quite different from those for Au–TiO_2 (Fig. 1). Results of the cycling experiments (Fig. 6) coupled with the FTIR data (Fig. 5) help explain the unusual shapes of the light-off plots for Au–TiO_2–In_2O_3. Because similar curves are obtained in the second and the third runs (Fig. 6), and because agglomeration of gold nanoparticles is irreversible [39], the transition from region I to region II (Fig. 4) did not arise from deactivation due to sintering. The repeatability of the reaction without deactivation (Figs. 6 and 9) suggests that these gold particles were relatively stable against sintering under our conditions. FTIR spectra (Fig. 5) show that carboxylate/carbonate surface species were formed within region II (Fig. 4) concomitant with the transition from region I to region II, suggesting that the activity may be affected by their formation, possibly due to blocking of key reaction sites [7,12,13]. These species were gradually decomposed at higher temperatures (Fig. 5), consistent with a modest increase in CO_2 formation, until a sharp rise in activity was observed above 264 °C (Fig. 4). Thus, the latter includes a contribution from the decomposition of these surface species. Results in Fig. 4 allow differentiation of the roles of gold and the oxide support [32,33]. Below ca. 300 °C, CO_2 formation occurred mainly on gold sites or at sites activated by Au; above ca. 300 °C, CO_2 formation arose mainly from reactions over the support. Results (Fig. 4) support the scheme that carbonate species formed on the support through interaction of CO with lattice oxygen atoms [28,32,33,40] and/or hydroxyl groups [9,41] have little (if any) contribution to CO_2 formation at low temperatures, but may inhibit CO oxidation (region I → region II).

The differences in the profiles for Au–TiO_2 (Fig. 1) and AuTiO_2–In_2O_3 lead to the suggestion that the surface species responsible for the region I → region II transition form as a result of differences in the nature of the TiO_2(P25) and TiO_2–In_2O_3 support materials, or that these surface species are less stable over titania (P25) and decompose rapidly. Despite the role of In_2O_3 in suppressing the anatase-phase → rutile-phase transformation of TiO_2, there was no evidence of compound formation between TiO_2 and In_2O_3, which is in accordance with previous observations for this composite oxide when heated to 1073 K [42]. Note that the surface of In_2O_3 had stronger Lewis acid sites than the surface of TiO_2 [42]; this may be significant in terms of the differences between P25 and TiO_2–In_2O_3. The longer breakthrough time for water over Au–TiO_2–In_2O_3 (Fig. 9) compared with Au–TiO_2 (Fig. 2) is consistent with the strong adsorption of molecular water at these Lewis acid centres.

It is clear that the Au–TiO_2–In_2O_3 may be further activated in a reaction mixture (Figs. 6 and 9). It is known that prolonged exposure to the reaction mixture may reduce ionic gold species to metallic gold [11]. Similarly, cooling in inert gas and detection of activity at room temperature above the level of a fresh, uncalcined sample (Figs. 1 and 6) provides further evidence against the need for oxidised Au surfaces for activity. In fact, cooling in either inert or in air had similar effects on the profile of the reused catalyst, leading to the conclusion that the state of the gold may not be the overriding factor leading to the loss of the contribution from gold at high temperature (region III) but recovery of activity at room temperature.

If CO and O_2 were competitively adsorbed on gold sites [32,33], then different initial activities from simultaneous and consecutive addition of reagents would be expected. Introducing CO for 5 min to a surface cooled in inert gas before introducing O_2 led to a rapid evolution of CO_2 (for the second and third runs) not found in the first run, in which the two reacting molecules were introduced simultaneously. This difference was seen within region I, in which the oxidation reaction is assumed to involve gold sites. To account for this competitive adsorption, a reaction pathway involving activation of CO on the surface and perimeter of gold particles and activation of oxygen at the perimeter interface to form OC–Au–O intermediate species has been proposed [32,33]. Results of CO adsorption on Au–TiO_2 suggest that CO can also adsorb at the gold–oxide interface [43]. Due to sequential addition of reacting molecules (Fig. 6), competitive adsorption of the two reacting species at the same gold sites does not offer a plausible explanation as to why more CO_2 evolved initially (for the second and the third runs), because the sites where the two reacting molecules compete (step sites closer to the borderline with the support [32,33]) and/or the perimeter interface or gold–oxide interface [43]) should be already populated by CO before the oxygen is introduced. Noting that first introducing CO onto the catalyst surface led to sites completely covered with CO and that there are virtually no sites for O_2 adsorption on gold sites, it was suggested on the basis of EPR experiments [44] that adsorption of CO reduces the TiO_2 support by eliminating oxide ions (lattice oxygen atoms) at the sites closest to the gold particles. Molecular oxygen is not adsorbed directly on gold particles, but is absorbed at the oxygen vacancy sites on oxide support adjacent to gold particles [28,40]. These considerations suggest that population of sites by CO molecules close to the interface with the support [43] leaves the surface of the oxide

support material (TiO_2–In_2O_3) as the site for molecular oxygen adsorption and activation.

Involvement of molecular oxygen may lead to the formation of carbonate species (CO_3^{2-}) [45]; however, in region I, the contributions of carbonate/carboxylate species to the formation of CO_2 were apparently negligible (Fig. 5), consistent with isotopic experiments results [28,46]. This rules out carbonate species as intermediates. Once such carbonates are formed, they are thermally stable [9] (Fig. 6) and may contribute to the plateau area in region II as a result of inhibition of the active Au-based sites. Reactions within regions I and II depended only on the concentration of Au–CO surface species, whereas above region III, the activity on the support alone coincided with that of Au–TiO_2–In_2O_3 catalyst, suggesting that reactions occurred over the support without participation of Au sites. Calcination of Au–Fe_2O_3 catalyst at 673 K led to a drastic decrease in the concentration of the surface OH/H_2O species [47,48], which affected catalyst activity. The reduced concentration of surface OH/H_2O species at high temperature (Fig. 5c–e) and the equivalent activity of Au–TiO_2–In_2O_3 and TiO_2–In_2O_3 support above region III are consistent with a scheme in which dehydroxylation diminishes the activity of Au–TiO_2–In_2O_3 to that of the TiO_2–In_2O_3 support alone. This proposed role of hydroxyl groups in the CO oxidation reaction over supported gold catalysts is consistent with previous findings [9,16,41,47,48]. This high-temperature loss of activity was reversible; activity was recovered after the catalyst was cooled to room temperature and was independent of the gaseous atmosphere used. The very different responses of Au–TiO_2 (Fig. 2) and Au–TiO_2–In_2O_3 (Fig. 10) to water vapour and the relative breakthrough times for detection of water vapour are consistent with the differing extent of hydrophilicity of the different supports and explain the lack of high-temperature deactivation exhibited by Au–TiO_2 (Fig. 1).

4.3. Influence of added water

The effect of water on the CO oxidation reaction over supported gold catalysts has been studied before, with conflicting results [7,8,14]. Irreversible deactivation of Au–TiO_2 due to the presence of moisture has been reported [7], in which removing water vapour from the feed did not restore the original activity, and activity could be restored only after calcination and reduction at 473 K. Grunwaldt et al. [8] observed reversible deactivation of Au–TiO_2 by water. Our results demonstrate (Figs. 2 and 10) that the effect of water on the activity for CO oxidation was reversible for both TiO_2–In_2O_3- and TiO_2 (P25)-supported Au catalysts. Our results also show that activity was recovered at a stage where the level of surface H_2O was still higher than at the beginning of the experiment and that activity could be fully recovered before water levels drop significantly (Fig. 2). For Au–TiO_2, the final activity was greater than the activity before water was added. The rise in activity to the original value (before the addition of water) while the H_2O level on the surface was still high (Fig. 11, curves b and g), the decrease in H_2O signal at the beginning (up to 27 min) with the rise in activity, and the rise in activity to greater than the original value before the addition of water (Fig. 2) suggest that H_2O- and/or H_2O-derived species may facilitate the formation of CO_2 [29] or contribute to producing an active catalyst surface. Excess water can significantly suppress the reaction, however. Results indicate that hydrogen oxidation is not of significance under these conditions, consistent with results of Schubert et al. [46], who observed a sharp decrease in H_2 oxidation in the presence of water. A proposed reaction mechanism for Au–TiO_2 involving the effect of water in the CO oxidation reaction [49] involves the dissociative adsorption of water on the TiO_2 surface, followed by the formation of the formate species (Au–$COOH^-$), which are decomposed to CO_2 and H_2. No spectral contributions due to formate or bicarbonate were detected here to support such a scheme, indicating that they were formed but in small concentrations and were rapidly decomposed or they were not formed at all. Because H_2 evolution was not accompanied by changes in the rate of CO_2 formation (Figs. 2 and 10), the latter is the preferred explanation.

Another important observation is the rise in hydrogen signal after the adsorption of water on the catalyst surface, suggesting hydrogen production during the reaction (Figs. 2 and 9). Date et al. [50] did not detect H_2 during similar experiments. H_2 evolution after the addition of water suggests that the catalysts may have been active for the water–gas shift reaction [49]. However, because the onset of H_2 after 70 min (Fig. 10) was not accompanied by a change in the rate of CO_2 formation, and because the rate of CO_2 formation increased when the H_2 signal began to level off after 119 min (Fig. 2) and after 139 min (Fig. 10) (i.e., recovery of activity was accompanied by a constant level of H_2 in the exit stream), it is unlikely that CO_2 and H_2 formation arose from the same reaction.

H_2O is adsorbed at coordinatively unsaturated Ti^{4+} sites on the surface of Au–TiO_2, because CO is readily displaced by exposure of H_2O to a CO-covered surface, and adsorbed CO is not detected after exposure of CO on a H_2O-covered surface [32]. For the same reason, H_2O apparently displaces CO from gold sites close to the gold–oxide interface [32]. The fact that the infrared band for CO molecules bound to atop sites on gold particles is detected after exposure of H_2O to a CO-covered surface and/or exposure of CO to a H_2O-preadsorbed surface [32,40] suggests that H_2O molecules may not prefer these atop sites on Au particles. In fact, this band due to CO on gold was red-shifted in the presence of H_2O and was explained in terms of the coadsorption of electron-rich species (H_2O and/or OH^-) on sites close to the gold–oxide interface [32]. Adsorption of H_2O molecules on oxygen vacancy sites reduces the concentration of oxygen vacancies and/or O_2^- superoxide radicals on the surface, which are required for CO oxidation, and is consistent with observed deactivation in the presence of excess H_2O and in line with the results of Date and Haruta [30], who demonstrated that large amounts of H_2O had a negative influence on the activity of Au/TiO_2 (P25) catalysts. The possible reactions that are considered important in these experiments and are consistent with our observations are shown in Scheme 1.

Exposure of molecular oxygen to defect-rich TiO_2 results in dissociation of O_2 at oxygen vacancy sites. One O atom fills the vacancy, whereas the other is bound to a Ti^{4+} site, which

(i) H_2O dissociation:

$$H_2O_{ads} + O_{ads} + H_2O_{ads} \rightarrow 2OH_{ads} + H_2O_{ads}, \quad (1)$$

$$H_2O_{ads} \rightarrow OH_{ads} + H_{ads}. \quad (2)$$

(ii) Combination of dissociated products:

$$H_{ads} + H_{ads} \rightarrow H_{2ads} \rightarrow H_2(g), \quad (3)$$

$$H_{ads} + O_{ads} \rightarrow OH_{ads}, \quad (4)$$

$$H_{ads} + OH_{ads} \rightarrow H_2O_{ads}, \quad (5)$$

$$2OH_{ads} \rightarrow O_{ads} + H_2O_{ads}, \quad (6)$$

$$CO_{ads} + O_{ads} \rightarrow CO_{2ads} \rightarrow CO_2(g). \quad (7)$$

(iii) Dissociation of molecular oxygen:

$$Ti^{4+}\left(^{+\delta}HOH^{\delta+}\right)\left(^{-\delta}O{=}O^{\delta-}\right) \rightarrow Ti^{4+}(OH)(OOH). \quad (8)$$

Scheme 1. Proposed reaction sequence showing the effect of water on the chemistry of the Au–TiO_2–In_2O_3 catalyst.

plays a role in the dissociation of H_2O [51]. During recombination of OH groups [reaction (6) in Scheme 1] and subsequent desorption of H_2O, the O_{ads} remains on the surface and can dissociate further H_2O molecules during repetitive adsorption and desorption experiments [51]. In reaction (1), the ratio of H_2O:O_2 is not 1:1, in accordance with experimental results for Pt(111) [52]. Theoretical projections suggest that the final state ($2OH + H_2O$) is more stable than the initial state ($2H_2O + O$) through hydrogen bonding interactions, resulting in a decreased reaction barrier; that is, the second H_2O molecule plays a catalytic role in OH formation [53]. This reaction channel is not the only one present, because it produces OH groups as its sole product, whereas H_2(g) was detected here (Figs. 2 and 11).

Oxygen vacancies may play a role in H_2O dissociation on rutile single crystals [54]. In some cases, H_2 was detected during desorption experiments after exposure of H_2O onto defect-rich TiO_2 surfaces [54]. The dissociated products (OH and H) are both bound to Ti^{4+} sites. Dissociation of H_2O has also been suggested for Au–TiO_2 and Au–ZnO, although uncoordinated gold sites are presumed responsible [32]. For Au–TiO_2, it has been suggested that the resulting H atoms from H_2O dissociation are stabilized on TiO_2 as O–H-localized groups; that is, atomic hydrogen is produced by coadsorption of CO–H_2O on Au–ZnO, but not on Au–TiO_2 [32].

From the foregoing observations [32,54], it is reasonable to assume that the introduction of water on the surface is initially dominated by dissociation [reactions (1) and (2) in Scheme 1]. Reaction (1) probably occurs at T^{4+}/In^{3+}, because O_{ads} [51] and H_2O molecules [32,51] are adsorbed on these sites. Reaction (2) occurs on oxygen vacancy sites and is stabilized on Ti^{4+} sites close to vacancy sites [51]. Because: (i) the presence of gold on the oxide surface facilitates the migration of oxygen vacancies from the bulk to the surface of oxide [55], (ii) CO molecules adsorbed on gold sites create oxygen vacancies by reacting with lattice oxygen atoms adjacent to the gold particles [44], and (iii) O_{ads} results from adsorption and dissociation of molecular oxygen at oxygen vacancy sites [51], reactions (1) and (2) also may occur at sites adjacent to gold particles. These reactions may proceed as long as oxygen vacancies and O_{ads} are available. Reactions (1) and (2) deplete the surface of O_{ads} and oxygen vacancy sites required for molecular oxygen activation (O_2^-) [28], which may explain in part the observed decrease in activity (Figs. 2 and 10). Note that reaction (4) also consumes O_{ads}, and its contribution to the activity drop may also be significant. Reaction (4) also increases the concentration of OH_{ads}. It is reasonable to assume that OH_{ads} and H_{ads} species dominate the first surface layer and that subsequent layers are dominated by molecularly adsorbed H_2O interacting through hydrogen bonding, as indicated by the growth of ν(O–H) at ca. 3400 cm^{-1} and δ(HOH) at ~1629 cm^{-1}. The latter finding confirms that H_2O is adsorbed molecularly [32].

Our results (Figs. 2 and 10) indicate that H atoms combine to form H_2(g), which desorbs along with H_2O molecules. Reaction (3) depletes the surface of H_{ads} and thus decreases the extent of reactions (4) and (5). Over time, possibly when the water vapour levels are sufficiently depleted, H_2 is desorbed together with undissociated H_2O (and/or recombined OH group) molecules [reaction (6)]. This continues until all of the H_2 is desorbed, as indicated by constant signal beyond 139 min, and the H_2O levels on the surface drop (Fig. 10). Note that some of the H_2O desorbing from the surface might arise from recombination of OH groups [reaction (6)]. As more H_2O molecules are removed, reaction (6) becomes favoured. Note that reaction (6) leaves O_{ads} on the surface, as suggested previously [51]; as more O_{ads} becomes available, reaction (7) is favoured, and thus recovery in activity occurs [point (e), Fig. 10]. This does not rule out the possibility that other mechanisms may contribute to CO_2 formation, however.

From the preceding discussion, because O_2^- molecules are stabilized on surface Ti^{4+} sites [28,40] and H_2O molecules are also adsorbed at these sites (Ti^{4+} ions) [32], it is possible, as was suggested before [51], that O_{ads} and H_2O molecules stabilize on surface Ti^{4+}, leading to reaction (1) and that O_2^- stabilized on these surface ions may abstract protons from H_2O molecules adsorbed at the same Ti^{4+} ion to form OOH radicals, as reflected in reaction (8). Similar species were proposed to arise from the interaction of the superoxo species adsorbed on metallic gold sites and H atoms of H_2O molecules in the gas phase, which provide oxygen for CO oxidation [56]. These are similar to the highly oxidizing intermediate radicals produced during photochemical decomposition of organic molecules on the surface of TiO_2 [57]. It is clear from reaction (8) that H_2O assists in dissociating the superoxide radical (O_2^-).

5. Conclusion

The Au–TiO_2–In_2O_3 catalyst exhibited lower CO oxidation activity than the benchmark Au–TiO_2 (P25) catalyst but was highly resistant to irreversible deactivation due to sintering even after reaction up to 500 °C. Characterization of the TiO_2–In_2O_3 composite oxides showed that the presence of In_2O_3 is highly dispersed through the anatase matrix and modifies the surface properties of titania. Pretreatment in different gaseous atmospheres have no significant influence on the performance of the Au–TiO_2–In_2O_3 catalyst for the CO oxidation reaction. The temperature-dependent activity curves for Au–

TiO_2–In_2O_3 and Au–TiO_2 (P25) were quite different. Light-off profiles were consistent with a scheme in which two independent reactions for CO_2 formation occur. At low temperatures ($\leqslant$264 °C), CO_2 formation occurred on gold sites but probably involved hydroxyl groups of the support. Dehydroxylation occurred more readily for TiO_2–In_2O_3 than for TiO_2 (P25) and led to reversible deactivation of the catalyst using the former as a support. At higher temperatures, CO_2 formation arose mainly from reaction over the support. Cooling in any gas led to recovery of activity at room temperature due to rehydroxylation of the support surface.

Acknowledgments

The authors thank the Royal Society (London) for supporting a study visit (for A.D.) and the Royal Society (London)/NRF (South Africa) for support under the joint collaborative programme involving the Universities of Aberdeen, Cardiff, and Witwatersrand. They also thank G. Rangel Porras for preparing the support material and Drs. Z. Liu and R. Daley for providing experimental assistance.

References

[1] M. Haruta, T. Kobayashi, H. Sano, N. Yamada, Chem. Lett. 2 (1987) 405.
[2] M. Haruta, Catal. Today 36 (1997) 153.
[3] G.C. Bond, D.T. Thompson, Catal. Rev.-Sci. Eng. 41 (1999) 319.
[4] M. Haruta, N. Yamada, T. Kobayashi, S. Ijima, J. Catal. 115 (1989) 301.
[5] A. Wolf, F. Schuth, Appl. Catal. A: Gen. 22 (2002) 1.
[6] G.B. Hoflund, S.D. Gardner, Langmuir 11 (1995) 3431.
[7] M.A. Bollinger, M.A. Vannice, Appl. Catal. B: Environ. 8 (1996) 417.
[8] J.D. Grunwaldt, C. Kiener, C. Vogerbaoer, A. Baiker, J. Catal. 181 (1999) 223.
[9] A. Knell, P. Barnickel, A. Baiker, A. Wokaun, J. Catal. 137 (1992) 306.
[10] D. Andreeva, Gold Bull. 35 (2002) 82.
[11] A.M. Visco, F. Neri, G. Neri, A. Donato, C. Milone, S. Galvagno, Phys. Chem. Chem. Phys. 1 (1999) 2869.
[12] G.Y. Wang, H.L. Lian, W.X. Zhang, D.Z. Jiang, T.H. Hu, Kinet. Catal. 43 (2002) 433.
[13] B. Schumacher, V. Plzak, M. Kinne, R.J. Behm, Catal. Lett. 89 (2003) 109.
[14] E.D. Park, J.S. Lee, J. Catal. 186 (1999) 1.
[15] M. Valden, X. Lai, D.W. Goodman, Science 281 (1998) 1647.
[16] C.K. Costello, S.-S. Oh, Y. Wang, M.C. Kung, H.H. Kung, Appl. Catal. A: Gen. 232 (2002) 159.
[17] A.M. Visco, F. Neri, A. Donato, C. Milone, S. Galvagno, Phys. Chem. Chem. Phys. 11 (1999) 2875.
[18] S. Minico, S. Scire, C. Cristafulli, A.M. Visco, S. Galvagno, Catal. Lett. 47 (1997) 273.
[19] A.I. Kozlov, A.P. Kozlova, H. Liu, Y. Iwasawa, Appl. Catal. A: Gen. 182 (1999) 9.
[20] F.E. Wagner, S. Galvagno, C. Melone, A.M. Visco, L. Stievano, S. Galgero, J. Chem. Soc. Faraday Trans. 93 (1997) 3403.
[21] A.P. Kozlova, S. Sugiyama, A.I. Koslov, K. Asakura, Y. Iwasawa, J. Catal. 176 (1998) 426.
[22] M. Haruta, S. Tsubota, T. Kobayashi, H. Kageyama, M.J. Genet, B. Delmon, J. Catal. 144 (1993) 175.
[23] M. Valden, S. Pak, X. Lai, D.W. Goodman, Catal. Lett. 56 (1998) 7.
[24] R. Zanella, S. Giorgio, C.-H. Shin, C.R. Henry, C. Louis, J. Catal. 222 (2004) 357.
[25] M.A.P. Dekkers, M.J. Lipits, B.E. Nieuwenhuys, Catal. Lett. 56 (1998) 195.
[26] S.D. Lin, M. Bollinger, M.A. Vannice, Catal. Lett. 17 (1993) 245.
[27] P. Landon, J. Ferguson, B.E. Solsona, T. Garcia, A.F. Carley, A.A. Herzing, C.J. Kiely, S.E. Golunski, G.J. Hutchings, Chem. Commun. (2005) 3385.
[28] H. Liu, A.I. Kozlov, A.P. Kozlova, T. Shido, K. Asakura, Y. Iwasawa, J. Catal. 185 (1999) 37.
[29] G.C. Bond, D.T. Thompson, Gold. Bull. 33 (2000) 41.
[30] M. Date, M. Haruta, J. Catal. 201 (2001) 221.
[31] M.S. Mallick, M.S. Scurrell, Appl. Catal. A: Gen. 253 (2003) 527.
[32] F. Boccuzzi, A. Chiorino, S. Tsubuta, M. Haruta, J. Phys. Chem. 100 (1996) 3625.
[33] M. Haruta, Catal. Surv. Jpn. 1 (1997) 61.
[34] M.M. Schubert, A. Venugopal, M.J. Kahlich, V. Plzak, R.J. Behm, J. Catal. 222 (2004) 32.
[35] K.K. Bando, K. Sayama, H. Kusama, K. Okabe, H. Arakawa, Appl. Catal. A: Gen. 165 (1997) 391.
[36] L. Guczi, G. Petö, A. Beck, K. Frey, O. Geszti, G. Molnár, C. Daróczi, J. Am. Chem. Soc. 125 (2003) 4332.
[37] P. Konova, A. Naydenov, Cv. Venkov, D. Mechandjiev, A. Andreeva, T. Tabakova, J. Mol. Catal. A: Chem. 213 (2004) 235.
[38] F. Moreau, G.C. Bond, A.O. Taylor, Chem. Commun. (2004) 1642.
[39] V.A. Bondzie, S.C. Parker, C.T. Campbell, Catal. Lett. 63 (1999) 143.
[40] H. Liu, A.I. Kozlov, A.P. Kozlova, T. Shido, Y. Iwasawa, Phys. Chem. Chem. Phys. 1 (1999) 2851.
[41] A.K. Tripathi, V.S. Kamble, N.M. Gupta, J. Catal. 187 (1999) 332.
[42] D. Shchukin, S. Poznyak, A. Kulak, P. Pichat, J. Photochem. Photobiol. A: Chem. 162 (2004) 423.
[43] S. Lee, C. Fan, T. Wu, S.L. Anderson, J. Am. Chem. Soc. 126 (2004) 5682.
[44] M. Okumura, J.M. Coronado, J. Soria, M. Haruta, J.C. Conesa, J. Catal. 203 (2001) 168.
[45] Z. Hao, L. Fen, G.Q. Lu, J. Liu, L. An, H. Wang, Appl. Catal. A: Gen. 213 (2001) 173.
[46] M. M Schubert, S. Hackenberg, A.C. van Veen, M. Muhler, V. Plzak, R.J. Behm, J. Catal. 197 (2001) 113.
[47] N.M. Gupta, A.T. Tripathi, Gold Bull. 34 (2001) 120.
[48] S.T. Daniels, M. Makkee, J.A. Moulijn, Catal. Lett. 100 (2005) 39.
[49] D. Andreeva, V. Idakiev, T. Tabakova, A. Andreev, R. Giovanoli, Appl. Catal. A: Gen. 134 (1996) 275.
[50] M. Date, S. Tsubota, M. Haruta, Angew. Chem. Int. Ed. 43 (2004) 2129.
[51] W.S. Epling, C.H.F. Peden, M.A. Hederson, U. Dibold, Surf. Sci. 412/413 (1998) 333.
[52] S. Volkening, K. Beduftig, K. Jacobi, J. Winterlin, G. Ertl, J. Chem. Phys. 111 (1999) 11147.
[53] X.-Q. Gong, P. Hu, R. Raval, J. Chem. Phys. 119 (2003) 6324.
[54] G. Lu, A. Linsebigler, J.T. Yates Jr, J. Phys. Chem. 98 (1994) 11733.
[55] J.A. Rodriquez, G. Liu, T. Jirsak, J. Habek, Z. Chang, J. Dvorak, A. Maiti, J. Am. Chem. Soc. 124 (2002) 5242.
[56] F. Boccuzzi, A. Chiorino, M. Manzoli, P. Liu, T. Akita, S. Ichikawa, M. Haruta, J. Catal. 202 (2001) 256.
[57] S. Wen, J. Zhao, G. Shen, J. Fu, P. Peng, Chemosphere 50 (2003) 111.